DOI: 10.1002/ejoc.201101623

A BODIPY-Based Highly Selective Fluorescent Chemosensor for Hg^{2+} Ions and Its Application in Living Cell Imaging

Mani Vedamalai[a] and Shu-Pao Wu*[a]

Keywords: Sensors / Mercury / Fluorescence / Imaging agents

A new boron–dipyrromethene (BODIPY) derivative (**FS1**) containing two triazole units exhibits an enhanced fluorescence in the presence of Hg^{2+} ions and a high selectivity for Hg^{2+} ions over competing metal ions in methanol: Ag^{+}, Ca^{2+}, Cd^{2+}, Co^{2+}, Cu^{2+}, Fe^{2+}, Fe^{3+}, K^{+}, Mg^{2+}, Mn^{2+}, Ni^{2+}, Pb^{2+}, and Zn^{2+} produced only minor changes in the fluorescence of **FS1**. The apparent dissociation constant (K_d) of **FS1**–Hg^{2+} was found to be 62 μM. Moreover, fluorescence microscopy experiments showed that **FS1** can be used as a fluorescent probe for detecting Hg^{2+} ions in living cells.

Introduction

Mercury is one of the most toxic heavy metal elements.[1] It exists in three different forms: Inorganic mercury, alkylmercury, and elemental mercury. Mercury contamination occurs through various processes, such as the combustion of fossil fuels, mining, and solid-waste incineration. Mercury ions show a high affinity for thiol groups in proteins, leading to the malfunction of cells and consequently causing many health problems in the brain, kidney, and central nervous system. Its accumulation in the body can contribute to the development of a wide variety of diseases, such as prenatal brain damage, serious cognitive and motion disorders, and Minamata disease.[2] Owing to the extreme toxicity of mercury, the United States Environmental Protection Agency (EPA) established the standard for the maximum allowed level of mercury in dietary and environmental sources to be 2 ppb (10 nM).

Numerous methods[3] for the detection of mercury ions in various samples have been proposed, including atomic absorption/emission spectroscopy,[4] inductively coupled plasma-mass spectroscopy (ICPMS),[5] inductively coupled plasma-atomic emission spectrometry (ICP-AES),[6] and voltammetry.[7] Most of these methods require expensive instruments and are not suitable for performing assays. Over the past decade more attention has been focused on the development of fluorescent chemosensors for the detection of Hg^{2+} ions.[8]

Because Hg^{2+} is known to be a fluorescence quencher, most fluorescent chemosensors detect Hg^{2+} by fluorescence quenching through spin–orbit coupling.[9] Owing to their sensitivity, fluorescent chemosensors that detect metal ions by fluorescence enhancement are more easily monitored than those that operate by fluorescence quenching. This paper reports on a newly designed BODIPY-based fluorescent enhancement chemosensor for Hg^{2+} based on photoinduced electron transfer (PET). The binding of Hg^{2+} to the chemosensor blocks the PET mechanism and greatly enhances the fluorescence of BODIPY.

In this work we designed a BODIPY-based fluorescent chemosensor for metal-ion detection. Two parts make up the chemosensor **FS1**: A BODIPY moiety as reporter and two triazole units that chelate the metal ion (Scheme 1). **FS1** exhibits weak fluorescence due to quenching by photoinduced electron transfer from the lone-pair electrons on the nitrogen atom attached to the phenyl group. The binding of metal ions to the chemosensor blocks the PET mechanism and results in considerable fluorescence enhancement of BODIPY. The metal ions Ag^{+}, Ca^{2+}, Cd^{2+}, Co^{2+}, Cu^{2+}, Fe^{2+}, Fe^{3+}, Hg^{2+}, K^{+}, Mg^{2+}, Mn^{2+}, Ni^{2+}, Pb^{2+}, and Zn^{2+}were tested for metal-ion-binding selectivity with **FS1**, but Hg^{2+} was the only ion that caused green emission upon binding with **FS1**.

Results and Discussion

Synthesis of FS1

The synthesis of **FS1** is outlined in Scheme 1. Aniline was treated with propargyl bromide in the presence of K_2CO_3 to afford compound **1**. Compound **2** was obtained by reaction of compound **1** with $POCl_3$ in the presence of

[a] Department of Applied Chemistry, National Chiao Tung University,
Hsinchu, Taiwan, Republic of China
Fax: +886-3-5723764
E-mail: spwu@mail.nctu.edu.tw

Supporting information for this article is available on the WWW under http://dx.doi.org/10.1002/ejoc.201101623.

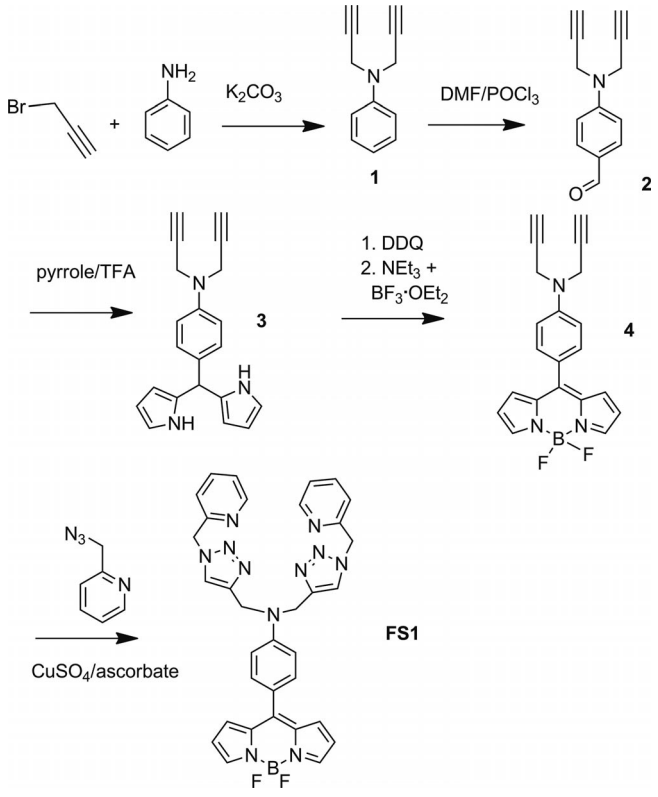

Scheme 1. Synthesis of **FS1**.

DMF at 80 °C. Treatment of compound **2** with excess pyrrole in the presence of TFA under nitrogen yielded the corresponding dipyrromethane **3**. In the next step, compound **3** was oxidized with DDQ to yield the corresponding dipyrromethene, which was transformed into the BODIPY skeleton **4** in the presence of BF_3 under N_2. Treatment of compound **4** with picolyl azide yielded **FS1** under click chemistry conditions. **FS1** has an absorbance maximum at 493 nm, assigned to the $S_0 \rightarrow S_1$ transition of the BODIPY chromophore,[10] and a molar extinction coefficient of 3.83×10^4 M^{-1} cm^{-1}. **FS1** displays weak fluorescence with a quantum yield of $\Phi = 0.002$, because photoinduced electron transfer from the aromatic amine group to the BODIPY moiety takes place.

Cation-Sensing Selectivity

The sensing ability of **FS1** was tested by mixing it with the metal ions Ag^+, Ca^{2+}, Cd^{2+}, Co^{2+}, Cu^{2+}, Fe^{2+}, Fe^{3+}, Hg^{2+}, K^+, Mg^{2+}, Mn^{2+}, Ni^{2+}, Pb^{2+}, and Zn^{2+}. Qualitatively, Hg^{2+} was the only ion that caused a change in color (from red to yellow) of the **FS1** solution and green fluorescence from **FS1** (Figure 1). Other metal ions had no significant effect on the fluorescence of **FS1**. Quantitative fluorescence spectra of **FS1** were recorded in the presence of several transition-metal ions. Hg^{2+} was the only metal ion that caused significant green emission (Figure 2). During the titration of **FS1** against Hg^{2+}, a new emission band centered at 520 nm was observed (Figure 3). After the addition of 4 equiv. of Hg^{2+}, the emission intensity reached a maximum. The quantum yield of the emission band was Φ = 0.035, which is 17-fold higher than that of **FS1**, with Φ = 0.002. These results indicate that Hg^{2+} is the only metal ion of those studied that readily binds to **FS1**, causing significant fluorescence enhancement and permitting the highly selective detection of Hg^{2+}.

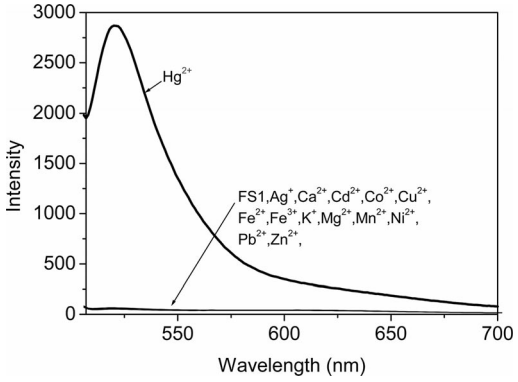

Figure 2. Fluorescence response of **FS1** (30 μM) to various metal cations (30 μM) in methanol. The excitation wavelength was 492 nm.

To study the influence of other metal ions on the binding of Hg^{2+} to **FS1**, we performed competitive experiments with Hg^{2+} (150 μM) and other metal ions (150 μM; Figure 4). The fluorescence enhancement observed for the mix-

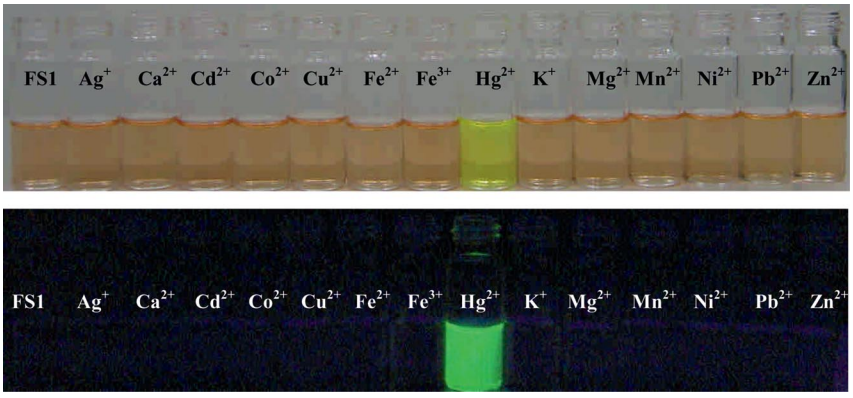

Figure 1. Color (top) and fluorescence (bottom) changes in **FS1** (30 μM) upon the addition of various metal ions (60 μM) in methanol.

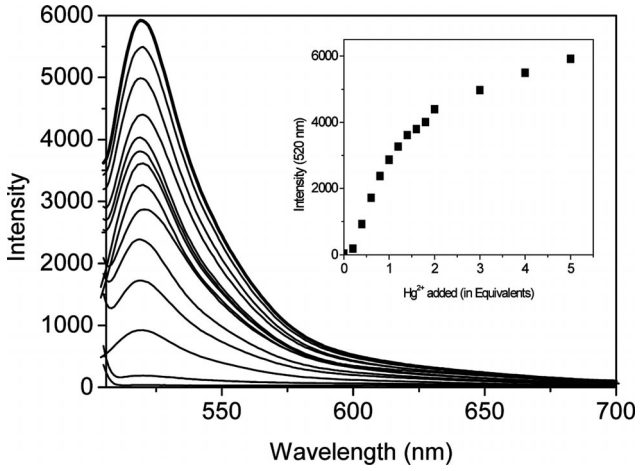

Figure 3. Fluorescence response of **FS1** (30 μM) to various equivalents of Hg^{2+} in methanol. The excitation wavelength was 492 nm.

tures of Hg^{2+} with most metal ions was similar to that caused by Hg^{2+} alone. Reduced fluorescence enhancement was observed when Hg^{2+} was mixed with Co^{2+} or Fe^{3+}. This indicates that only Co^{2+} and Fe^{3+} compete with Hg^{2+} for binding with **FS1**. Most of the other metal ions do not interfere with the binding of **FS1** to Hg^{2+}.

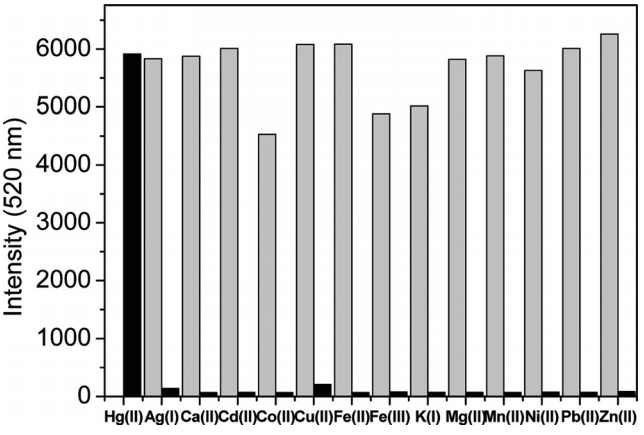

Figure 4. Fluorescence response of **FS1** (30 μM) to Hg^{2+} (150 μM) and other metal ions (150 μM; black bars) and to mixtures of Hg^{2+} (150 μM) with other metal ions (150 μM; gray bars) in methanol.

To determine the binding stoichiometry of the **FS1**–Hg^{2+} complex, the emission intensity of **FS1** at 520 nm was plotted as a function of the molar fraction of **FS1** under a constant total concentration. The resulting Job plot is shown in Figure 5. The maximum emission intensity was reached when the molar fraction was 0.5, which indicates a 1:1 ratio for the **FS1**–Hg^{2+} complex, that is, one Hg^{2+} ion binds to one molecule of **FS1**. Furthermore, the formation of a 1:1 **FS1**–Hg^{2+} complex was confirmed by ESI-MS, in which the peak at m/z = 828.1 indicates a 1:1 stoichiometry for the **FS1**–Hg^{2+} complex (see Figure S9 in the Supporting Information). The apparent dissociation constant was calculated from Figure 3 by using a nonlinear regression analysis; a value of 62.1 ± 5.7 μM was determined (see Figure S10 in the Supporting Information). The detection limit of **FS1** as a fluorescent sensor for the analysis of Hg^{2+} was determined from the variation of fluorescence intensity as a function of the concentration of Hg^{2+} (see Figure S12 in the Supporting Information). It was found that **FS1** has a detection limit of 2.8 μM, which allows micromolar concentrations of Hg^{2+} to be detected.

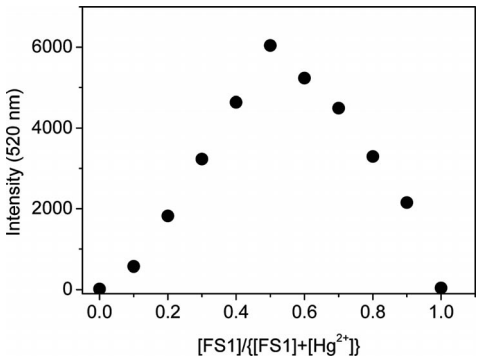

Figure 5. Job plot of **FS1**–Hg^{2+} complexes in methanol. The solutions were monitored at a wavelength of 520 nm. The total concentration of the sensor and Hg^{2+} ion was 250 μM.

To gain a clearer understanding of the structure of the **FS1**–Hg^{2+} complex, ^1H NMR spectroscopy (Figure 6) was employed. Hg^{2+} is a heavy metal ion and can affect the proton signals that are close to the Hg^{2+} binding site.[11] The ^1H NMR spectra of **FS1** recorded with increasing amounts of Hg^{2+} show that the proton (H_g, triazole) signal at δ = 7.8 ppm is shifted downfield as Hg^{2+} is added. This indicates that Hg^{2+} binds to **FS1** mainly through the nitrogen atom in the triazole ring. The proton signals H_e and H_d are shifted upfield upon addition of Hg^{2+}. This also indicates that Hg^{2+} binds through the amino group attached to the phenyl ring. The proton signals from H_i, H_j, H_k, and H_l on the pyridine ring are slightly affected by the binding of Hg^{2+}. These observations show that Hg^{2+} binds to **FS1** through an amino group, two nitrogen atoms of two triazole units, and two pyridine nitrogen atoms.

A pH titration of **FS1** was carried out to investigate a suitable pH range for Hg^{2+} sensing. As depicted in Figure 7, the emission intensities of metal-free **FS1** are very low at all pH values. After mixing **FS1** with Hg^{2+}, the emission intensity at 520 nm is markedly higher at pH = 5.0 and is a maximum in the pH range 5.0–10.0. At pH > 10, the emission intensity decreases. This indicates poor stability of the **FS1**–Hg^{2+} complexes at high pH values. At pH < 5, the emission intensity is also lower due to the protonation of the amino groups, which prevents the formation of the **FS1**–Hg^{2+} complex.

Living Cell Imaging

FS1 was also used for living cell imaging. For the detection of Hg^{2+} in living cells, HeLa cells were treated with 20 μM $Hg(BF_4)_2$ for 30 min and washed with phosphate-buffered saline (PBS) three times. Then the cells were incubated with **FS1** (20 μM) for 30 min and washed with PBS to

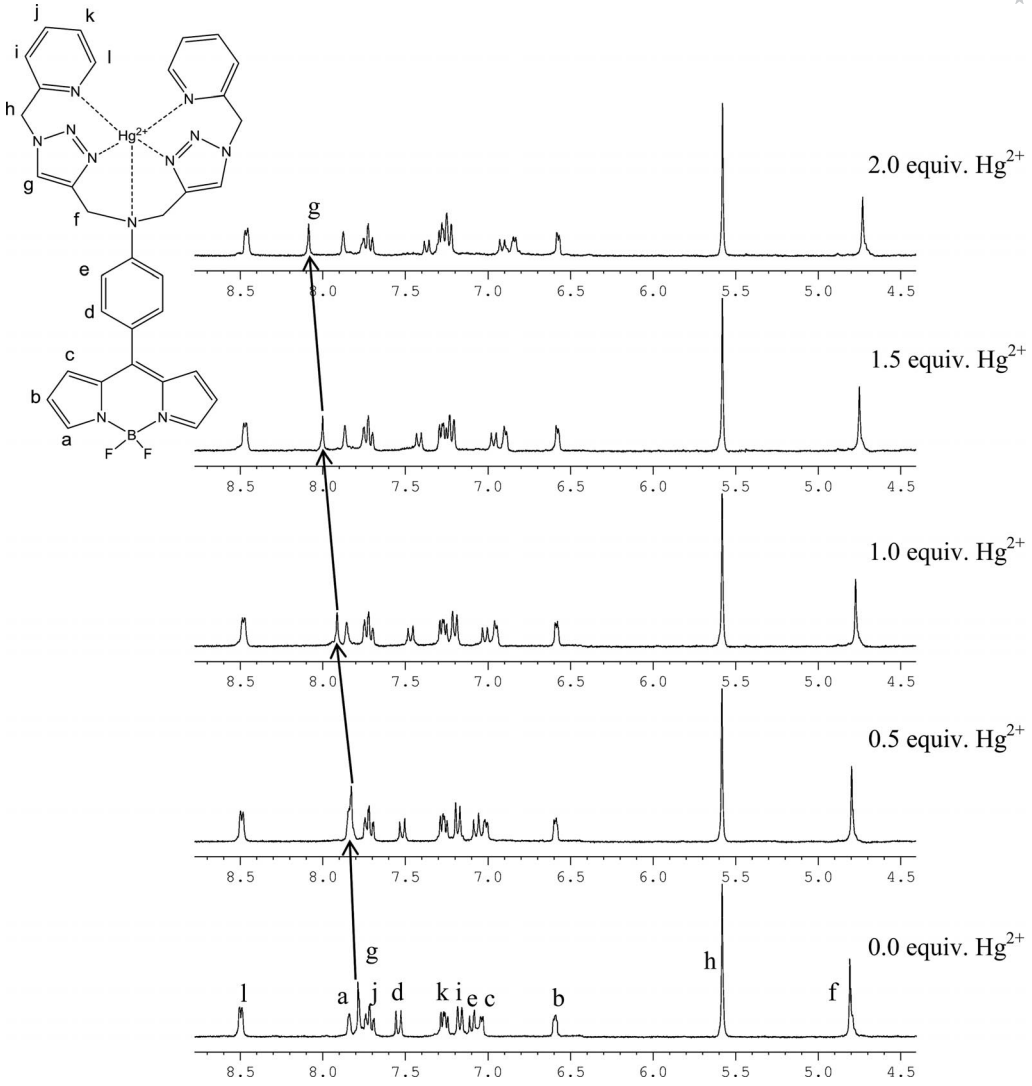

Figure 6. ^1H NMR spectra of **FS1** (5 mM) in the presence of different concentrations of Hg^{2+} in CD_3CN.

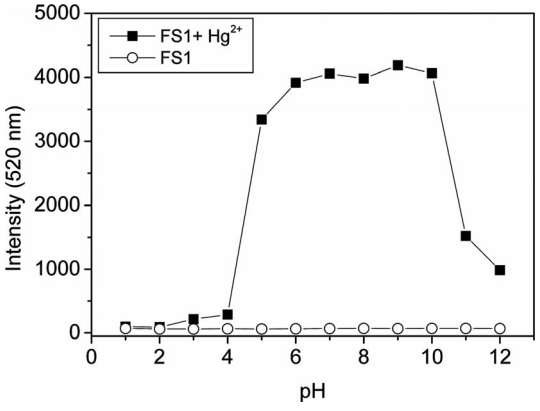

Figure 7. Fluorescence intensity (520 nm) of free **FS1** (30 μM; ○) and of **FS1** after the addition of Hg^{2+} (150 μM; ■) in methanol/water solution (9:1, v/v; 1 mM buffer) as a function of the pH. The excitation wavelength was 492 nm. Buffer solutions: pH = 1–2, KCl/HCl; pH = 2.5–4, KHP/HCl; pH = 4.5–6, KHP/NaOH; pH = 6.5–12 HEPES.

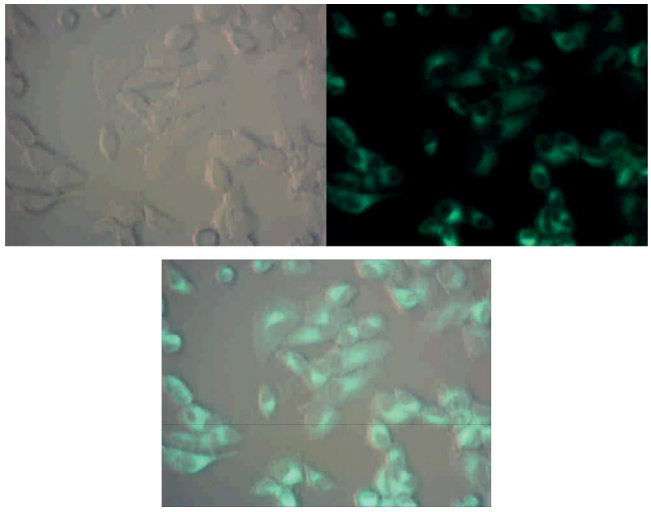

Figure 8. Hg^{2+}-treated HeLa cell images. Top left: bright-field image; top right: fluorescence image; bottom: merged image.

remove any remaining sensor. Images of the HeLa cells were obtained with a fluorescence microscope. Figure 8 shows the images of the HeLa cells with **FS1** after treatment of Hg^{2+}. The overlapping of the fluorescence and bright-field images reveals that the fluorescence signals are localized in the intracellular area, which indicates a subcellular distribution of Hg^{2+} and good permeability of the cell membrane of **FS1**.

Conclusions

The new fluorescence chemosensor **FS1** exhibits a high affinity and selectivity for Hg^{2+} ions over competing metal ions. The fluorescence of **FS1** was significantly enhanced in the presence of Hg^{2+}, and the addition of Ag^{+}, Ca^{2+}, Cd^{2+}, Co^{2+}, Cu^{2+}, Fe^{2+}, Fe^{3+}, K^{+}, Mg^{2+}, Mn^{2+}, Ni^{2+}, Pb^{2+}, or Zn^{2+} barely affected the fluorescence. This BODIPY-based Hg^{2+} chemosensor is also an effective method for Hg^{2+} sensing in living cell imaging.

Experimental Section

General: All solvents and reagents were obtained from commercial sources and used as received without further purification. UV/Vis spectra were recorded with an Agilent 8453 UV/Vis spectrometer. Fluorescence spectra were recorded with a Hitachi F-4500 spectrometer. ^1H and ^{13}C NMR spectra were recorded with a Bruker DRX-300 NMR spectrometer.

Synthesis of *N*,*N*-Diprop-2-ynylaniline (1): Compound **1** was obtained in modest yield by treating aniline with propargyl bromide in the presence of potassium carbonate.[12]

Synthesis of 4-(Diprop-2-ynylamino)benzaldehyde (2): Phosphorus oxychloride (306.7 mg, 2 mmol) was added dropwise to a solution of compound **1** (338.2 mg, 2 mmol) in DMF (2 mL), and the mixture was then heated at 90 °C for 3 h. After cooling to ambient temperature, the reaction mixture was dissolved in CH_2Cl_2 (100 mL) and washed with a dilute sodium hydrogen carbonate solution. The solvent was evaporated under reduced pressure, and the crude product was purified by column chromatography (ethyl acetate/hexane, 1:10) to give compound **2** as a white solid. Yield: 354.7 mg (90%); m.p. 54–55 °C. ^1H NMR ($CDCl_3$): δ = 9.82 (s, 1 H), 7.81 (d, J = 8.7 Hz, 2 H), 6.96 (d, J = 8.7 Hz, 2 H), 4.22 (d, J = 2.4 Hz, 4 H), 2.30 (t, J = 2.4 Hz, 2 H) ppm. ^{13}C NMR ($CDCl_3$): δ = 191.0, 152.2, 132.2, 127.9, 113.7, 78.7, 73.6, 40.5 ppm. MS (EI): m/z (%) = 197 (100.0), 172 (13.86), 167 (58.54), 132 (19.59). HRMS (EI): calcd. for $C_{13}H_{11}NO$ 197.0841; found 197.0838.

Synthesis of 4-[Bis(1*H*-pyrrol-2-yl)methyl]-*N*,*N*-diprop-2-ynylaniline (3): Trifluoroacetic acid (TFA, 0.1 mL) was added to a solution of compound **2** (296 mg, 1.5 mmol) in pyrrole (2 mL). The solution was stirred under nitrogen at room temperature for 4 h, and the reaction was then quenched with 0.1 M sodium hydroxide. The organic phase was extracted with ethyl acetate and dried with anhydrous $MgSO_4$. The solvent was evaporated under reduced pressure, and the crude product was purified by column chromatography (ethyl acetate/hexane, 3:10) to give compound **3** as a yellowish viscous liquid. Yield: 389.9 mg (83%). ^1H NMR ($CDCl_3$): δ = 7.91 (s, 2 H), 7.13 (d, J = 8.7 Hz, 2 H), 6.91 (d, J = 8.7 Hz, 2 H), 6.67–6.69 (m, 2 H), 6.15 (q, J = 2.7 Hz, 2 H), 5.91–5.94 (m, 2 H), 5.42 (s, 1 H), 4.11 (d, J = 2.4 Hz, 4 H), 2.25 (t, J = 2.4 Hz,2 H) ppm. ^{13}C NMR ($CDCl_3$): δ = 146.4, 133.1, 132.8, 129.0, 117.0, 115.6, 108.1, 106.9, 79.1, 72.8, 42.9, 40.4 ppm. MS (FAB): m/z = 313. HRMS (FAB): calcd. for $C_{21}H_{19}N_3$ 313.1579; found 313.1578.

Synthesis of 4,4-Difluoro-8-[4-(*N*,*N*-diprop-2-ynylamino)phenyl]-4-bora-3a,4a-diaza-*s*-indacene (4): 2,3-Dichloro-5,6-dicyano-1,4-benzoquinone (DDQ; 318 mg, 1.4 mmol) dissolved in CH_2Cl_2 (50 mL) was added to a solution of compound **3** (376 mg, 1.2 mmol) in CH_2Cl_2 (100 mL) under nitrogen, and the mixture was stirred for 3 h. It was then treated with Et_3N (4 mL) and $BF_3{\cdot}OEt_2$ (5 mL) for 12 h. The solvent was evaporated under reduced pressure, and the crude product was purified by column chromatography (ethyl acetate/hexane, 1:10) to give compound **4** as an orange solid. Yield: 258.6 mg (60%); m.p. 226–227 °C. ^1H NMR ($CDCl_3$): δ = 7.90 (s, 2 H), 7.58 (d, J = 8.7 Hz, 2 H), 7.02–7.05 (m, 4 H), 6.55 (d, J = 2.4 Hz, 2 H), 4.24 (d, J = 2.4 Hz, 4 H), 2.33 (t, J = 2.4 Hz, 2 H) ppm. ^{13}C NMR: δ = 149.7, 147.8, 142.6, 134.6, 132.6, 131.1, 124.2, 118.0, 113.7, 78.4, 73.1, 40.2 ppm. MS (FAB): m/z = 359. HRMS (FAB): calcd. for $C_{21}H_{16}BF_2N_3$ 359.1405; found 359.1407.

Synthesis of 4,4-Difluoro-8-[4-(*N*,*N*-bis{[1-(pyridin-2-ylmethyl)-1*H*-1,2,3-triazol-4-yl]methyl}amino)phenyl]-4-bora-3a,4a-diaza-*s*-indacene (FS1): Picolyl azide (180 mg, 1.34 mmol), $CuSO_4{\cdot}5H_2O$, (16.8 mg, 10 mol-%), and sodium ascorbate (26.6 mg, 20 mol-%) were added to a solution of compound **4** (240.6 mg, 0.67 mmol) in THF/H_2O (7:3, v/v; 15 mL) under nitrogen. The solution was stirred at room temperature for 12 h. A saturated ammonium chloride solution (20 mL) was added to the reaction mixture, and the organic phase was extracted with dichloromethane (10 mL, 3×). The combined organic extracts were dried with anhydrous $MgSO_4$. The solvent was evaporated under reduced pressure, and the crude product was purified by column chromatography (dichloromethane/methanol, 6:1) to give compound **FS1** as a dark-red solid. Yield: 320.0 mg (76%); m.p. 145–146 °C. ^1H NMR (CD_3CN): δ = 8.50 (d, J = 4.2 Hz, 2 H), 7.84 (s, 2 H), 7.79 (s, 2 H), 7.72 (dt, J = 1.8, 7.5 Hz, 2 H), 7.53 (d, J = 9.0 Hz, 2 H), 7.26 (dd, J = 4.8, 7.5 Hz, 2 H), 7.18 (d, J = 7.8 Hz, 2 H), 7.09 (d, J = 8.7 Hz, 2 H), 7.03 (d, J = 3.9 Hz, 2 H), 6.59 (dd, J = 2.1, 4.1 Hz, 2 H), 5.58 (s, 4 H), 4.81 (s, 4 H) ppm. ^{13}C NMR (CD_3CN): δ = 155.7, 151.8, 150.4, 149.2, 145.2, 142.5, 138.0, 134.9, 134.0, 131.8, 124.4, 124.0, 122.9, 122.8, 118.7, 113.4, 55.8, 46.8 ppm. MS (ESI): m/z = 628.3 $[M + H]^+$. HRMS (ESI): calcd. for $C_{33}H_{29}BF_2N_{11}$ $[M + H]^+$ 628.2669; found 628.2678.

Determination of the Binding Stoichiometry and the Apparent Dissociation Constants for the Binding of Hg^{II} to FS1: The binding stoichiometry of the **FS1**–Hg^{2+} complex was determined from a Job plot. The fluorescence intensity at 520 nm was plotted against the molar fraction of **FS1** with a total concentration of the sensor and Hg^{2+} ion of 250 μM. The molar fraction at maximum emission intensity represents the binding stoichiometry of the **FS1**–Hg^{2+} complex. The maximum emission intensity was reached at a molar fraction of 0.5 (Figure 4). This result indicates that chemosensor **FS1** forms a 1:1 complex with Hg^{2+}. The apparent dissociation constant (K_d) was calculated by nonlinear regression analysis.[13] The plot was fitted with normalized fluorescence emission intensity against the concentration of the Hg^{2+} ion according to Equation (1) in which F is the fluorescence intensity at 520 nm at any given Hg^{2+} concentration, F_{min} is the fluorescence intensity at 520 nm in the absence of Hg^{2+}, F_{max} is the maximum fluorescence intensity at 520 nm in the presence of Hg^{2+}, n is the number of Hg^{2+} ions bound per probe molecule, and K_d is the dissociation constant: n = 1 according to the Job plot.

$$F = (F_{max}[Hg^{2+}]^n + F_{min}K_d)/(K_d + [Hg^{2+}]^n) \quad (1)$$

Cell Culture: The cell line HeLa was provided by the Food Industry Research and Development Institute (Taiwan). The HeLa cells were grown in DMEM supplemented with 10% FBS at 37 °C and 5% CO_2. Cells were plated on 14 mm glass coverslips and allowed to adhere for 24 h.

Fluorescence Imaging: HeLa cells were cultured in Dulbecco's modied Eagle's medium (DMEM) supplemented with 10% fetal bovine serum (FBS) at 37 °C under an atmosphere of 5% CO_2. Cells were plated on 14 mm glass coverslips and allowed to adhere for 24 h. Experiments to assess the Hg^{2+} uptake were performed in phosphate-buffered saline (PBS) with 20 μM $Hg(BF_4)_2$. The cells were treated with 10 mM solutions of $Hg(BF_4)_2$ (2 μL; final concentration: 20 μM) dissolved in sterilized PBS (pH = 7.4) and incubated at 37 °C for 30 min. The treated cells were washed with PBS (3 × 2 mL) to remove remaining metal ions. Culture medium (2 mL) was added to the cell culture, which was then treated with a 10 mM solution of chemosensor **FS1** (2 μL; final concentration: 20 μM) dissolved in DMSO. The samples were incubated at 37 °C for 30 min. The culture medium was removed, and the treated cells were washed with PBS (3 × 2 mL) before observation. Fluorescence imaging was performed with a ZEISS Axio Scope A1 fluorescence microscope. Cells loaded with **FS1** were excited at 480 nm by using a 50 W Hg lamp. An emission filter of 535 nm was used.

Supporting Information (see footnote on the first page of this article): ^1H and ^{13}C NMR spectra of compounds **2**, **3**, **4**, and **FS1**; ESI-MS of **FS1**–Hg^{2+}.

Acknowledgments

We gratefully acknowledge the financial support of the National Science Council (ROC) and National Chiao Tung University.

[1] a) D. W. Boening, *Chemosphere* **2000**, *40*, 1335–1351; b) J. M. Benoit, W. F. Fitzgerald, A. W. Damman, *Environ. Res.* **1998**, *78*, 118–133; c) A. Renzoni, F. Zino, E. Franchi, *Environ. Res.* **1998**, *77*, 68–72; d) H. H. Harris, I. J. Pickering, G. N. George, *Science* **2003**, *301*, 1203.

[2] a) T. Takeuchi, N. Morikawa, H. Matsumoto, Y. Shiraishi, *Acta Neuropathol.* **1962**, *2*, 40–57; b) M. Harada, *Crit. Rev. Toxicol.* **1995**, *25*, 1–24.

[3] K. Leopold, M. Foulkes, P. Worsfold, *Anal. Chim. Acta* **2010**, *663*, 127–138.

[4] a) Y. Gao, S. De Galan, A. De Brauwere, W. Baeyens, M. Leermakers, *Talanta* **2010**, *82*, 1919–1923; b) M. J. da Silva, A. P. S. Paim, M. F. Pimentel, M. L. Cervera, M. de la Guardia, *Anal. Chim. Acta* **2010**, *667*, 43–48.

[5] a) F. Moreno, T. Garcia-Barrera, J. L. Gomez-Ariza, *Analyst* **2010**, *135*, 2700–2705; b) M. V. B. Krishna, K. Chandrasekaran, D. Karunasagar, *Talanta* **2010**, *81*, 462–472; c) W. R. L. Cairns, M. Ranaldo, R. Hennebelle, C. Turetta, G. Capodaglio, C. F. Ferrari, A. Dommergue, P. Cescon, C. Barbante, *Anal. Chim. Acta* **2008**, *622*, 62–69.

[6] X. Chai, X. Chang, Z. Hu, Q. He, Z. Tu, Z. Li, *Talanta* **2010**, *82*, 1791–1796.

[7] a) X. Fu, X. Chen, Z. Guo, C. Xie, L. Kong, J. Liu, X. Huang, *Anal. Chim. Acta* **2011**, *685*, 21–28; b) F. Wang, X. Wei, C. Wang, S. Zhang, B. Ye, *Talanta* **2010**, *80*, 1198–1204.

[8] a) X. Guo, X. Qian, L. Jia, *J. Am. Chem. Soc.* **2004**, *126*, 2272–2273; b) J. Wang, X. Qian, *Chem. Commun.* **2006**, 109–111; c) M. Yuan, Y. Li, J. Li, C. Li, X. Liu, J. Lv, J. Xu, H. Liu, S. Wang, D. Zhu, *Org. Lett.* **2007**, *9*, 2313–2316; d) A. Coskun, M. D. Yilmaz, E. U. Akkaya, *Org. Lett.* **2007**, *9*, 607–609; e) M. H. Lee, S. W. Lee, S. H. Kim, C. Kang, J. S. Kim, *Org. Lett.* **2009**, *11*, 2101–2104; f) J. Fan, K. Guo, X. Peng, J. Du, J. Wang, S. Sun, H. Li, *Sens. Actuators B* **2009**, *142*, 191–196; g) V. Bhalla, R. Tejpal, M. J. Kumar, A. Sethi, *Inorg. Chem.* **2009**, *48*, 11677–11684; h) K. G. Vaswani, M. D. Keranen, *Inorg. Chem.* **2009**, *48*, 5797–5800; i) N. Wanichacheva, M. Siriprumpoonthum, A. Kamkaew, K. Grudpan, *Tetrahedron Lett.* **2009**, *50*, 1783–1786; j) J. Du, J. Fan, X. Peng, P. Sun, J. Wang, H. Li, S. Sun, *Org. Lett.* **2010**, *12*, 476–479; k) W. Shi, S. Sun, X. Li, H. Ma, *Inorg. Chem.* **2010**, *49*, 1206–1210; l) S. Atilgan, T. Ozdemir, E. U. Akkaya, *Org. Lett.* **2010**, *12*, 4792–4795; m) O. A. Bozdemir, R. Guliyev, O. Buyukcakir, S. Selcuk, S. Kolemen, G. Gulseren, T. Nalbantoglu, H. Boyaci, E. U. Akkaya, *J. Am. Chem. Soc.* **2010**, *132*, 8029–8036.

[9] D. S. McClure, *J. Chem. Phys.* **1952**, *20*, 682–686.

[10] a) W. Qin, T. Rohand, W. Dehaen, J. N. Clifford, K. Driesen, D. Beljonne, B. Van Averbeke, M. Van der Auweraer, N. Boens, *J. Phys. Chem. A* **2007**, *111*, 8588–8597; b) A. Loudet, K. Burgess, *Chem. Rev.* **2007**, *107*, 4891–4932.

[11] M. Kaupp, O. L. Malkina, V. G. Malkin, P. Pyykko, *Chem. Eur. J.* **1998**, *4*, 118–126.

[12] N. G. Kundu, B. Nandi, *J. Org. Chem.* **2001**, *66*, 4563–4575.

[13] S. C. Dodani, Q. He, C. J. Chang, *J. Am. Chem. Soc.* **2009**, *131*, 18020–18021.

Received: November 10, 2011
Published Online: January 4, 2012

